Springer

KSME

Journal of Mechanical Science and Technology 29 (5) (2015) 1941~1953
www.springerlink.com/content/1738-494x
DOI 10.1007/s12206-015-0415-4

Crashworthy capacity of a hybridized epoxy-glass fiber aluminum columnar tube using repeated axial resistive force †

Perowansa Paruka[1,*], Waluyo Adi Siswanto[2], Md Abdul Maleque[3] and Mohd Kamal Mohd Shah[4]

[1]*Department of Mechanical Engineering, Politeknik Kota Kinabalu, Jalan Politeknik, Menggatal, 88450 Kota Kinabalu, Sabah, Malaysia*
[2]*Faculty of Mechanical and Manufacturing Engineering, Universiti Tun Hussein Onn Malaysia, 86400 Parit Raja, Batu Pahat, Johor, Malaysia*
[3]*Department of Manufacturing and Materials Engineering, Kuliyyah of Engineering, Universiti Islam Antarabangsa Malaysia, 53100 Kuala Lumpur, Malaysia*
[4]*Mechanical Engineering Program, Faculty of Engineering, Universiti Malaysia Sabah, Jalan UMS, 88400 Kota Kinabalu, Sabah, Malaysia*

(Manuscript Received May 28, 2014; Revised November 21, 2014; Accepted January 9, 2015)

Abstract

A combination of aluminum columnar member with composite laminate to form a hybrid structure can be used as collapsible energy absorbers especially in automotive vehicular structures to protect occupants and cargo. A key advantage of aluminum member in composite is that it provides ductile and stable plastic collapse mechanisms with progressive deformation in a stable manner by increasing energy absorption during collision. This paper presents an experimental investigation on the influence of the number of hybrid epoxy-glass layers in overwrap composite columnar tubes. Three columnar tube specimens were used and fabricated by hand lay-up method. Aluminum square hollow shape was combined with externally wrapped by using an isophathalic epoxy resin reinforced with glass fiber skin with an orientation angle of 0°/90°. The aluminum columnar tube was used as reference material. Crushed hybrid-composite columnar tubes were prepared using one, two, and three layers to determine the crashworthy capacity. Quasi-static crush test was conducted using INSTRON machine with an axial loading. Results showed that crush force and the number of layers were related to the enhancement of energy absorption before the collapse of columnar tubes. The energy absorption properties of the crushed hybrid-composite columnar tubes improved significantly with the addition of layers in the overwrap. Microscopic analysis on the modes of epoxy-glass fiber laminate failure was conducted by using scanning electron microscopy.

Keywords: Epoxy-glass fiber skin; Aluminum columnar; Hybrid materials; Crashworthy response; Quasi-static axial crushing; Performance properties

1. Introduction

Considerable research and development have been conducted to design safe automotive vehicular structures in recent decades. Reducing the weight of structures, which mainly utilize internal combustion engines, is important to optimize exhaust gas and to enhance the fuel economy target [1]. In connection with this need, lightweight materials, such as aluminum, can be utilized. Aluminum alloy has been extensively used in vehicular components, such as pistons, engine blocks, chassis, hoods, fenders, and doors. However, aluminum parts are difficult to produce because aluminum exhibits strain concentration and low ductility. A considerable amount of electrical energy and large facilities are also needed because of the poor spot welding characteristics of aluminum.

Composite material is another lightweight material. This material is a combination of two or more chemically distinct and insoluble phases with a recognizable interface, such that its properties and structural performance are superior to those of the constituents that act independently. These combinations are known as metal-matrix and ceramic-matrix composites, which are heterogeneous and anisotropic materials. Owing to these combinations, recycling used composite materials and designing composite structures are difficult. Meanwhile, fiber-reinforced composite materials are essentially used in automotive vehicular cabs and interior components, such as seats and paneling, because of their good resistance to corrosion during their in-service life, competitive cost, high specific strength, high damping capability, and high stiffness ratios coupled with a low specific weight, especially at elevated temperatures [2]. If composite materials are applied to vehicles, not only the weight of the vehicles is decreased but also their noise and vibration [3].

In a continuous manufacturing process for the production of composite structures and materials, large statistical variations occur in their mechanical properties, which might be due to uncertainties in the volume fraction of the resin content, the degree of cure and process-induced residual stresses during

*Corresponding author. Tel.: +60 88 499980, Fax.: +60 88 499960
E-mail address: perowansaparuka@yahoo.com, perowansa@polikk.edu.my
† Recommended by Associate Editor Vikas Tomar

composite manufacturing, the probability of defects and void formations inside the composites, and so on [4, 5]. Hence, a probabilistic or reliability analysis of the composite failure or the manufacturing process conditions and the product quality is needed [6, 7]. Such an analysis plays a vital role in strength evaluation of composite structures. In contrast to the deterministic analysis of composite materials, probabilistic analysis provides a better understanding of the effect of the variations inherently involved in geometry, material properties, or manufacturing process [7]. The latter makes it easier or more practical to predict how sensitive the scatter of the output parameters is, for example, the composite performance, failure criterion, and cure degree, with respect to the input design parameters [8]. The general mechanical behavior of a composite material is orthotropic, that is, transversely isotropic if only unidirectional fibers are used, and the coefficient of thermal expansion of polymer-matrix materials is usually higher than that of fibers [9]. A way for an evaluation of the robustness of the process is also provided.

When more than one type of material is utilized in a reinforced structure, the structure is known as hybrid. Hybrids generally have better properties than single-material structures, but they are more costly. For example, hybrid composites are anisotropic, that is, heterogeneous materials with significant properties in one or two directions, which do not deform plastically and are attractive structural materials in the form of a fiber-reinforced polymer-matrix composite wrap. In these cases, composites are primarily specified because they can be used to produce cost-effective, lightweight components of relatively complex geometries [10, 11]. Hybrid composites can be routinely applied to engineering structures for rebuilding and new construction of piles, piers, and columns, including in manufacturing plants, bridges, high-rise buildings, and harbors. They achieve a balance among stiffness, high strength, high ductility, membrane-related mechanical properties, and formwork-free construction [12-14]. Hybrid-composite materials not only have better mechanical qualities than other metallic materials for specific strength and fatigue characteristic but could also be manufactured in accordance with the needs of the user, such as increasing the strength by changing the fiber orientations along the axis of the structures [15-17].

Numerous researchers have investigated the axial crushing behavior of metal/composite hybrid tubes; they have shown that various factors and parameters, including geometry and shape, stacking sequence of composite lay-up, metal surface treatment, loading speed, foam filling, and specimen length, contribute to the collapse of hybrid tubes and affect the crashworthiness characteristics [16]. Huang et al. [17] and El-Hage et al. [18] numerically studied the axial crushing of circular and square hybrid tubes and showed that the best orientation angle for fiber ply orientation pattern was hoop reinforcement. Bouchet et al. [19] reported the effect of the surface treatment of metal tube prior to composite layer bonding on the energy absorption capability.

A large number of quasi-static crushing investigations have been conducted on metal/composite hybrid tubes, in which fiber-reinforced polymer is combined with metallic tubes to improve their mechanical properties and to evaluate the influence of fiber reinforcement on crush response [19, 20]. Shin et al. [21] performed quasi-static axial crush and bending collapse tests on hybrid tubes produced by wrapping glass fiber/epoxy prepregs around square aluminum tubes. The ply orientations were 0°, 90°, 0°/90°, and ±45° to the tube axis. The mean crush force and energy absorption capacity of the hybrid tubes were higher than those of the aluminum tubes. Song et al. [22] conducted quasi-static and impact tests on hybrid tubes of E-glass fiber/epoxy-wrapped aluminum, steel, and copper circular tubes. The fiber orientation angles in the overwrap were either ±15°, ±45°, or 90°. They reported the effects of such factors as strain rate, composite wall thickness, fiber ply orientation pattern, and mechanical properties of metal tube. They also reported the four main collapse modes for hybrid tubes, such as compound diamond, compound fragmentation, delamination, and catastrophic failure. Hanefi and Wierzbicki [23] proposed an analytical model for the estimation of the mean axial crush force of circular steel tubes externally overwrapped with hoop-wound composite layers, in which the core ply orientation of fiberglass angle was 90°. They assumed that the folding mode of some hybrid tubes was symmetric and matched existing ones of steel tube. The mean crush force and specific energy absorption increased with steel shell thickness and overwrap thickness.

The utilization of different triggering mechanisms on energy absorption characteristics has been investigated [24, 25]. Bevel triggers with a 45° chamfer around one tip end of pure aluminum columnar tube itself and hybrid-composite tube edges are widely used [23-30].

This study conducted experimental quasi-static crush tests on samples of pure aluminum columnar tube and hybrid aluminum-composite columnar tubes with three different thicknesses of reinforcing composites. Many important features of the columnar tube crush response were identified. The crushability of aluminum columnar itself and the fracture of the composite layers were considered through representative photos and scanning electron microscopy (SEM) micrographs. The performance properties of hybrid aluminum-composite columnar tube specimens were compared with those of a pure aluminum columnar tube specimen to evaluate the crashworthy capacity of hybridized epoxy-glass fiber aluminum columnar members. The results exploited by this work would be useful to enhance essential data needed for proper construction and effective design architecture of composite structural members in terms of plastically collapsing (Aluminum) and fracturing (External reinforcement) columnar tubes, as well as ease of actual crashworthy applications.

2. Materials and methodology

2.1 Specimen fabrications

The specimens used in this study were extruded aluminum

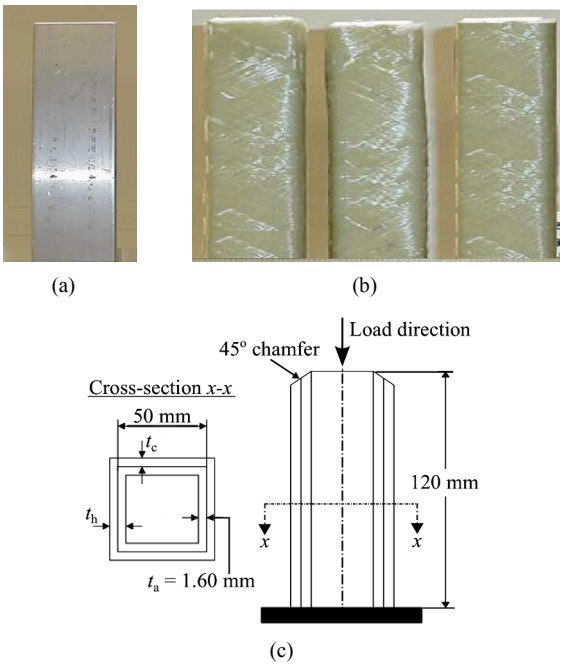

Fig. 1. Preparation of test specimens: (a) aluminum columnar tube; (b) hybrid aluminum-composite columnar tubes; (c) schematic views of a columnar tube (t_a = aluminum wall thickness, t_c = composite wall thickness, t_h = hybrid wall thickness).

columnar and hybrid-composite columnars made with a combination of an aluminum square hollow section and an external protection using isophathalic epoxy resin reinforced with glass fiber skin, as shown in Figs. 1(a) and (b). The materials used were as follows: (i) EN-AW7108-T6 aluminum alloy extrusion for columnar tubes; (ii) SE4849 Type 30 E-glass carbon fiber rovings (Owens corning); (iii) Shell Epon 828 epoxy resin and shell Epikure-cure curing agent W.

The aluminum columnar tube was obtained from a local market. Three hybrid columnars were fabricated by hand lay-up process with different layers of composite overwrap. Each layer was constructed by filament winding continuous glass fiber-epoxy composite prepregs overwrapped into an aluminum columnar tube. The main ply orientation of the fiber angle in the overwrap was [0°/90°] or unidirectional with respect to the axis of the longitudinal tube. The aluminum tube walls were not cleaned or treated with any chemicals prior to filament winding. The filament-wound hybrid tubes were cured completely before being extracted in an air circulating oven under 7×10^5 Nm^{-2} for 235 min at a temperature of 120°C. The process was conducted in accordance with the recommended curing cycle of the manufacturer.

Fig. 2 shows the cured cycle for the epoxy-glass fiber composite. During curing, the tube was slowly rotated to ensure even distribution of matrix around the tube. After curing the composite overwrap, the columnar hybrid tubes were cut to a length of 120 mm by using a diamond-tipped cutting wheel. Both ends of the tube were faced off to make them perpendicular to the tube axis. A bevel trigger with a 45° chamfer angle was machined onto one loading end of each tube edges to function as a crush initiator. The overwrap thickness was controlled by varying the number of layers in the reinforcement. Each layer consisted of multiple windings or back and forth passes to cover the mandrel surface with crisscrossed fiber banding.

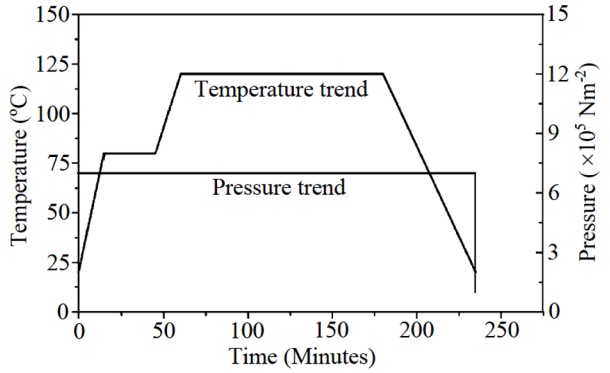

Fig. 2. Cured cycle of the epoxy-glass fiber hybrid materials of test specimens.

Section layers also existed in the tube wall. One was cross-wind fibers in approximately 0.25 mm of the glass fiber-epoxy composite thickness, measured from the inner width. The other one was glass strand matt on the outer width of the columnar tube to hold the unidirectional glass fibers during the hand lay-up process. The specimens were grouped into four different categories on the basis of their number of layers and thickness to analyze the performance level. Four specimens were used, and each specimen was screened before the test. They were designated as ACT0L (50 mm square), HCCT1L (55.52 mm square), HCCT2L (57.90 mm square), and HCCT3L (59.74 mm square) and then weighted. ACT0L was also represented as non-layered ("0L") aluminum columnar tube ("ACT"), whereas HCCT1L was indicated as hybrid-composite columnar tube ("HCCT") with one layer ("1L"). These columnar tube specimens had external width-to-wall thickness ratios of 31.25, 12.73, 10.43, and 9.23, which correponded to specimens ACT0L, HCCT1L, HCCT2L, and HCCT3L, respectively. Table 1 shows the dimensions of the overwrap thickness and the mass per unit length of the materials.

2.2 Experimental crush test procedures

All specimens were tested axially at room temperature using a computer-controlled INSTRON universal testing machine (Model type: MTS 8100 AG-I) with 100 kN maximum load capacity of an eccentric compressive head of upper platen [19]. Prior to the test, the rigid steel platens were lubricated to avoid any radial frictional forces caused by flexure. An axial crush force was then applied progressively over the top end of the nominal width of the hybrid aluminum-composite columnar tube specimen with a crosshead speed maintained at 6.75 mm/min until specimen failure. The force-deformation

Table 1. Geometrical details of the fabricated aluminum hybrid-composite columnar specimens.

Description	Specimen designation	No. of lay-up in the overwrapped	Aluminum wall thickness, t_a(mm)	Composite wall thickness, t_c(mm)	Hybrid wall thickness, $t_h = t_a + t_c$(mm)	Mass per length (g/mm)
Aluminum columnar	ACT0L	-	1.60	-	$t_h = t_a$=1.60	0.654
Hybrid-composite columnars	HCCT1L	1	1.60	2.76	4.36	0.782
	HCCT2L	2	1.60	3.95	5.55	0.926
	HCCT3L	3	1.60	4.87	6.47	1.069

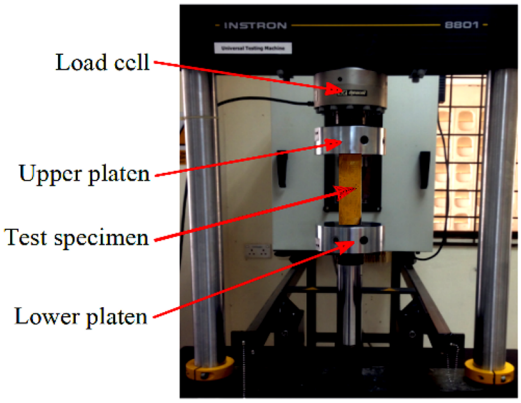

Fig. 3. Principle of crush test set-up at INSTRON machine.

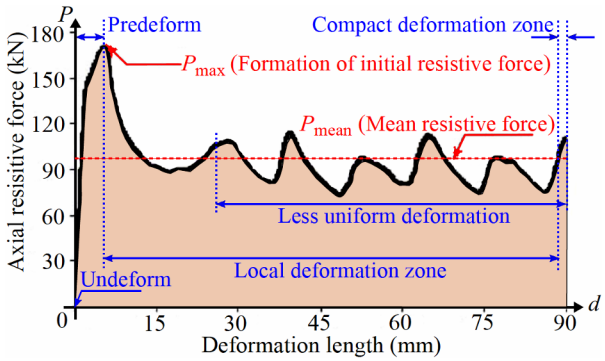

Fig. 4. Schematic diagram of typical force-deformation profile in quasi-static experimental crush test.

values were recorded automatically through the integrated data acquisition set-up.

Fig. 3 shows the test arrangement of a quasi-statically crushed hybrid-composite columnar tube. The tube was placed between the parallel rigid steel platen of the test machine without any additional clamping. The load signal was captured directly by a computer through a load cell connected to the machine. For each tube, quasi-static crush testing was conducted three times for repeatability or to evaluate the tendency of experimental results.

The crush performance data and axial resistive force-deformation curves of equivalent specimens were obtained using Fig. 4. The shaded area under the curve, such as crush absorbed energy, and maximum peak crush force on the curve, namely, maximum compressive-resistance force, were calculated. The following crashworthiness parameters were measured. The crush responses were obtained with mean crush force, P_{mean}, as the mean of all forces, and maximum resistive force, P_{max}, as the folding initiation force or in many cases as the initial peak force. This maximum resistive force, P_{max}, was divided by the cross-sectional area of the columnar tube specimen to gain the specific resistive force. The force can be computed using Eq. (1).

$$P_{specific} = \frac{P_{max}}{A}. \tag{1}$$

Crush force efficiency is the ratio of mean crush force and maximum crush force to evaluate the performance of a structure during the crush process [Eq. (2)].

$$\eta_c = \frac{P_{mean}}{P_{max}} \times 100\%. \tag{2}$$

The shaded area under the plotted force-deformation curve can be represented as a value of the total energy absorbed (Fig. 4). The total crush absorbed energy was determined by integrating the test data for the entire test period from 0 mm up to approximately 80 mm crush distance, as shown in Eq. (3), with d_{max} as the maximum deformation length.

$$E_{total} = \int_0^{d_{max}} P(s)\,ds. \tag{3}$$

This energy was divided by the mass of the crushed portion of the tube specimen to obtain the specific crush energy absorbed. This factor is the most important in designing any structures that need a reduced weight, such as automobiles and aircrafts. This factor can be computed using Eq. (4), with m_1 as the mass of the columnar tube.

$$E_{specific} = \frac{E_{total}}{m_1}. \tag{4}$$

All aluminum columnar tube and hybrid aluminum-composite columnar tube specimens were constrained to deform in the axial crush resistive force direction up to 80 mm

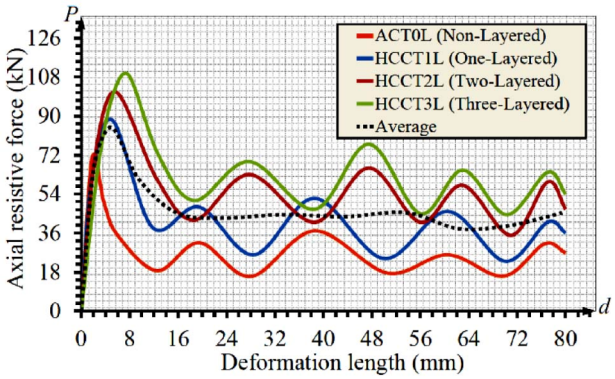

(a) Comparative average of force-deformation properties of different columnar tube specimens

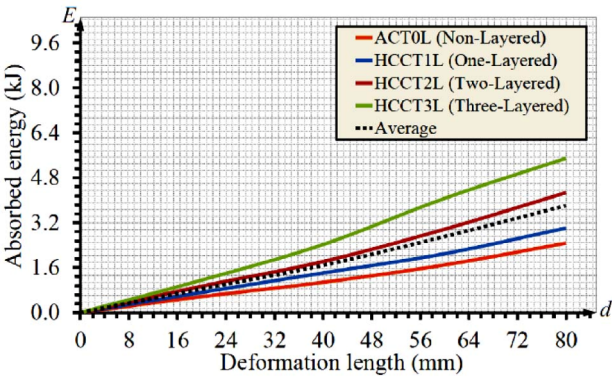

(b) Comparative average of energy-deformation properties of different columnar tube specimens

Fig. 5. Comparison of force-deformation plots and comparison of energy-deformation characteristics of hybrid aluminum-composite specimens.

deformation length. Finally, different modes of deformation and failure mechanisms, such as folding, buckling, bending, cracking, and delaminating, were examined by SEM.

3. Results and discussion

3.1 Experimental results of tested specimens

Force-deformation and energy-deformation curves related to different columnar tube specimens were extracted to clearly compare the crashworthiness properties of all columnar tube specimens. The obtained results of the force-deformation plot of each specimen through experiments were correlated with the different phases of deformation modes and failure mechanisms of each tested specimen. Fig. 5 shows the comparison of average force-deformation curve and energy-deformation characteristics of the results of the four tested specimens through experimental procedures.

Fig. 5(a) shows the increase and decrease in crush resistive force levels. The initial phase of the increased crush resistive force corresponded to the pre-buckling stage of collapse, whereas the structure offered a minimum deformation length with maximum crush resistive force or high load resistance. The corresponding crush resistive force level was designated as the first peak crush resistive force. Once the structure attained its first peak crush resistive force, it exhibited a non-linear mode of collapse and offered a reduced level of crush resistive force until the subsequent peak crush resistive force. The corresponding stage of collapse was termed as buckling, in which the axially crushed specimen began to collapse from the top nominal width toward the axis of axial crush direction.

The post-buckling stage of collapse followed after the buckling, in which the deformation rate of laminate over the buckled regions was non-linear in trend. The corresponding stage of force-deformation curve showed significant crush resistive force fluctuations. A similar trend was observed in all force-deformation plots. The positive slope of the oscillation of force-deformation plots indicated the progressive mode of the collapse of the hybrid aluminum-composite columnar tube. The amount of deformation and force-deformation characteristics showed that the hybrid-composite structures exhibited a non-linear mode of collapse with brittle-type fracture indications on the crushed regions. A comparison between force-deformation curves of the aluminum columnar tube and hybrid aluminum-composite columnar tubes indicated that the maximum peak crush resistive force in the aluminum columnar tube ACT0L was 70.64 kN less than those of the hybrid aluminum-composite columnar tubes HCCT1L, HCCT2L, and HCCT3L with the same length of 120 mm. Fig. 5(a) indicates that the mean crush resistive forces of the aluminum columnar tube ACT0L and the hybrid aluminum-composite columnar tubes HCCT1L, HCCT2L, and HCCT3L were 28.95, 39.91, 50.33, and 63.53 kN, respectively.

As shown in Fig. 5(b), a comparison between the energy-deformation curves of the aluminum columnar tube and hybrid aluminum-composite columnar tubes indicated that the energy absorption of the aluminum columnar tube ACT0L was 2475.07 J lower than those of the hybrid aluminum-composite columnar tubes HCCT1L, HCCT2L, and HCCT3L when the deformation length of 80 mm was reached. Therefore, with a combination of these tubes, the energy absorption of the hybrid aluminum-composite columnar tubes was greater than that of the aluminum columnar tube. The aluminum columnar tube was crushed primarily because its maximum peak crush resistive force was low. The energy absorption of the hybrid aluminum-composite columnar tubes, especially HCCT3L, was greater than that of the aluminum columnar tube itself.

As a result, the pure aluminum columnar tube had lower energy absorption and initial peak crush resistive force than the hybrid aluminum-composite columnar tubes. However, the energy absorption of the hybrid aluminum-composite columnar tubes was higher than that of the pure aluminum columnar tube itself. Many automotive industries use an aluminum columnar tube as front space frame to absorb crash energy. Strict safety standards nowadays have precipitated the development of a hybridized energy absorber with high energy absorption and low initial peak crush resistive force.

Table 2. Failure mechanisms of each fabricated hybrid aluminum-composite columnar tube specimen during progressive deformation.

Specimen designation	Type of mode of failure at every expected peak crush resistive force				
	Maximum peak crush resistive force	1st peak crush resistive force	2nd peak crush resistive force	3rd peak crush resistive force	4th peak crush resistive force
ACT0L	Buckling	Folding patterns	Splitting	Small wrinkles	Compacting
HCCT1L	Buckling	Frond bending	Splitting	Matrix cracking	Delamination
HCCT2L	Buckling	Frond bending	Splitting	Matrix cracking	Delamination
HCCT3L	Buckling	Frond bending	Splitting	Matrix cracking	Delamination

3.2 Progressive deformation of hybrid aluminum-composite columnar tubes

Representative photographs of the axial crush force on aluminum hybrid-composite columnar tubes were taken during the quasi-static experimental crush test, as shown in Figs. 6-9(a). The crushing behavior, deformation patterns, and amount of energy absorption of the specimens were investigated. The influences of crashworthiness parameters of aluminum hybrid-composite materials on these properties were studied. The representative photographs of triggered specimens were categorized as non-layered, one-layered, two-layered, and three-layered in the overwrapped thickness. The photographs presented the steps of the transient deformation process in the columnar tubes and were taken at different phases during the test. The corresponding axial crush resistive force-deformation plots and the corresponding energy-deformation characteristics of all the columnar tube series are shown in Figs. 6-9(b) and in Figs. 6-9(c), respectively. The curves marked with peak crush resistive force were correlated with the representative specimen photos for convenience in viewing the progress of the progressive crushing force.

Fig. 6 shows the representative photographs of the quasi-statically crush test of non-layered aluminum columnar tube (ACT0L). The development of the folding shapes was analyzed to determine the influence of the transient deformation process on the initiation of buckling, location of wrinkles, and their dependence on the crashworthy response. This response was the characteristics of progressive buckling once the structure folded sequentially [20]. The specimen buckled in dropped off resistive force started at the first peak resistive force of deformed distance from top end. The specimen buckled inward and generated axisymmetric folds with a uniform lob pattern during quasi-static axial crushing. Owing to continuous loading, the specimen deformed further gradually through rolling plastic deformation and generated stationary hinges with longitudinal cracks at four sharp corners. The formation of stationary hinges and axial cracks was always perpendicular to the direction of loading axis of rigid platens. The stress concentration at four corners caused tearing in the corner from top wall until the final buckling pattern with a 80 mm crush distance. This phenomenon is shown in Fig. 6(a). The strain propagation in the direction of loading can be followed when analyzing these patterns because of the dominance of the crushing force during the initial phase of deformation. Owing to the formation of crack stationary, the deformation process was in progressive axisymmetric mode.

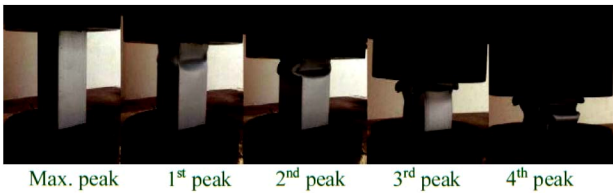

(a) Photographs of different phases or progressive deformation

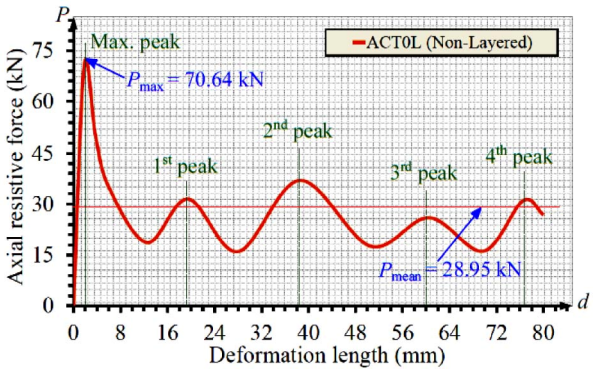

(b) Force-deformation curve of experimental results

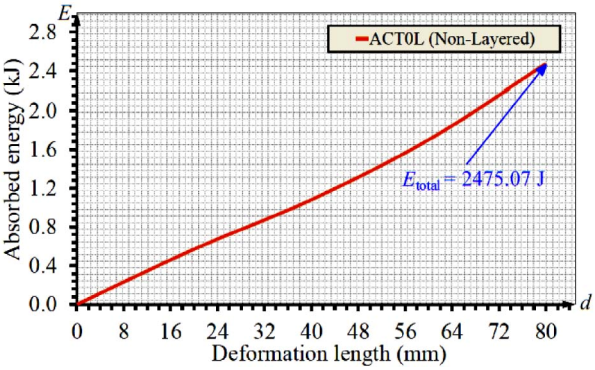

(c) Energy-deformation curve of experimental results

Fig. 6. Axial crush test of a non-layered specimen, ACT0L.

The axial crush force against crush deformation curve shown in Fig. 6(b) rapidly increased to a maximum peak resistive force significantly and then remained relatively constant. Given that no layer was present in the columnar tube ACT0L, the maximum resistive force was reached rapidly. However, after the first peak crush force was attained, the asymmetric

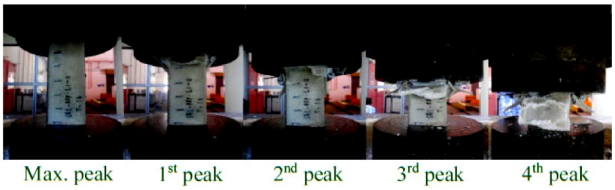

(a) Photographs of different phases or progressive deformation

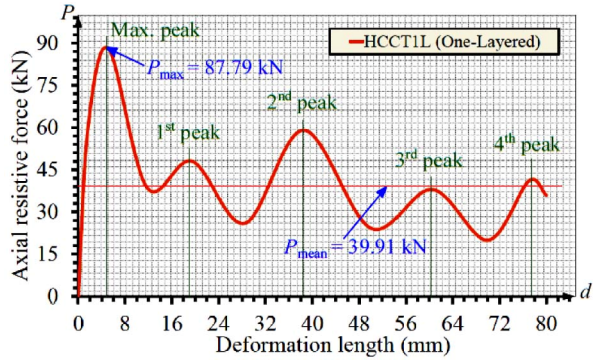

(b) Force-deformation curve of experimental results

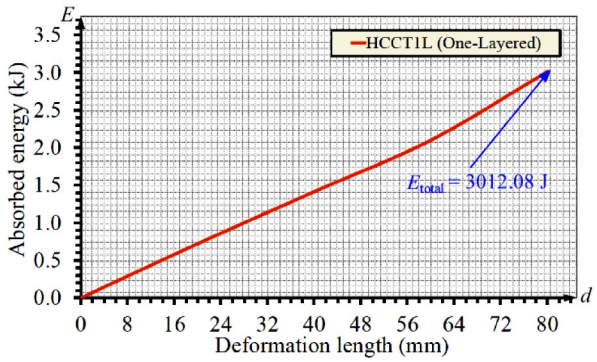

(c) Energy-deformation curve of experimental results

Fig. 7. Axial crush test of a one-layered specimen, HCCT1L.

folding pattern was completely initiated in the aluminum shell. The folding could continue dramatically when the progressive deformation proceeded with oscillating values of a small resistive force.

Fig. 7 shows the representative photos of one-layered epoxy-glass fiber hybrid-composite columnar tube, HCCT1L. In this case, the specimen crushed with regular asymmetric folds, frond bending, and post-buckling of deformation mode, as shown in Fig. 7(a). The initial phases of crushing showed circumferential delamination. A small wedge from debris was formed on top wall, and major crack developed in the mid-wall thickness. The wrapped composite material was constrained into folds of the aluminum tube. The fibers splitted toward the inner and outer, thereby resulting in the separation of two materials at the interface. Small-amplitude wrinkles were also observed along the deformation length of the columnar structures. This phenomenon is known as plastically rolling of deformation when the initial asymmetric folding pattern of columnar tube develops within a sustained plastic flow.

Fig. 7(b) shows the axial crush force against the crush deformation curve from the quasistatic crush test of one-layered specimen. In general, the characteristic of force-deformation history of one-layered specimen was different from that of nonlayered specimen. HCCT1L showed the typical deformation patterns, such as delamination, longitudinal splitting, and frond bending. Furthermore, a small amount of fiber fractures was also observed because of the significantly low number of composite layups. The gradual facilitation of one layer in HCCT achieved a linearly increased mean crushing force after a deformation length of 80 mm. However, initial peak crushing force was observed in the curve of the one-layered specimen. This peak crushing force was caused by fiber cracking formation and changing of deformation process mode from progressive asymmetric to nonsymmetric folding pattern as specimen collapse proceeded. Specimen collapse occurred completely after the first and maximum crushing forces. The required second peak crushing force for test continuation was abruptly reduced as a result of folding pattern formation in ACT. As failure progressed, another folding of lob patterns was formed from the part of the hybrid columnar tube that remained intact. This lob pattern showed the second peak crushing force. However, this lob pattern was not as smooth as that formed in the pure ACT because of microcrack propagation in the composite material. Hence, the second peak crushing force was remarkably smaller than the first peak crushing force. This observation also showed low efficiency in improving crashworthy capacity.

Fig. 8 shows the representative photos of two-layered epoxy-glass fiber HCCT, namely, HCCT2L, under quasistatic loading. This specimen was crushed with stable fronds at catastrophic mode of deformation in the HCCT. The deformation pattern of this specimen matched that of HCCT1L. Fig. 8(a) illustrates an irregular nonsymmetric (or nonuniform) deformation, which formed as columnar length buckled toward inner and outer width and resulted in separation of two materials at the interface. The initial phases of crushing force showed progressive crushing of triggering profile, which led to circumferential delamination. The later phases of the crushing force showed a sudden growth and propagation of longitudinal cracks at its major width location because of the higher radial stress concentration at that location. As a result of this phenomenon, the composite wall segment underwent post-buckling mode, thereby influencing improved crushing force. Subsequently, the fibers at the major width location were subject to fracture surface in collapse mode. The influence of these deformation patterns on the crushing force can be seen in Fig. 8(a). The stacking sequence of formation of the stationary cracks at the top wall cross section and the subsequent region of fiber surfaces were extended to the next major width location of the HCCT.

Fig. 8(b) plots the axial crush force against the crush deformation curve of the two-layered specimen. The plots revealed that oscillations were followed by maximum and initial peak crush force. The force deformation history of this HCCT

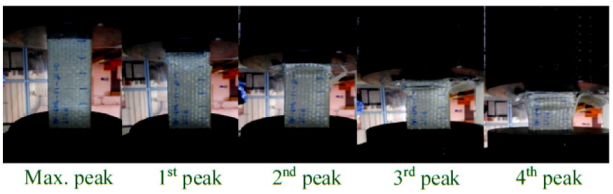

(a) Photographs of different phases or progressive deformation

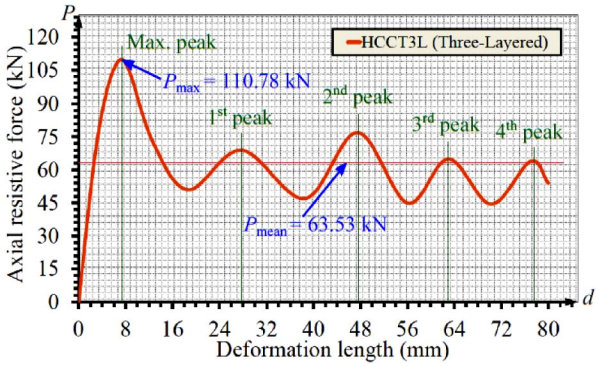

(b) Force-deformation curve of experimental results

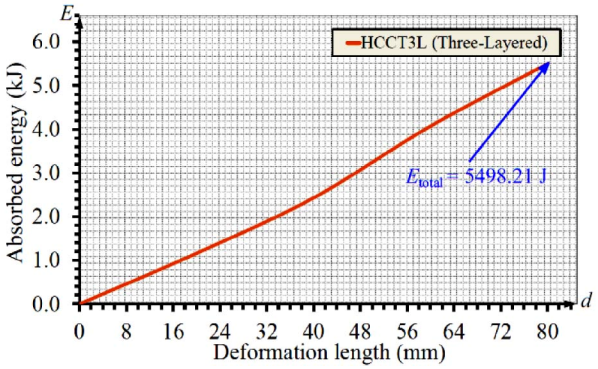

(c) Energy-deformation curve of experimental results

Fig. 8. Axial crush test of a two-layered specimen, HCCT2L.

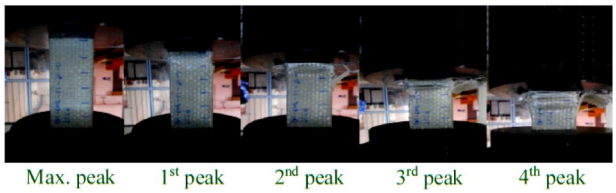

(a) Photographs of different phases or progressive deformation

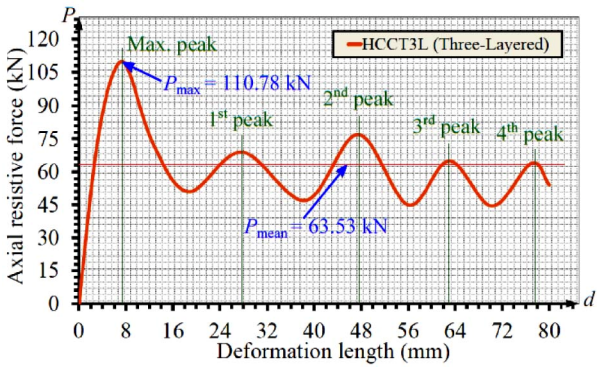

(b) Force-deformation curve of experimental results

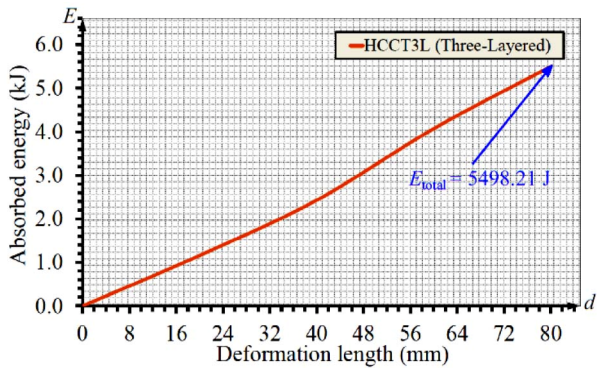

(c) Energy-deformation curve of experimental results

Fig. 9. Axial crush test of a three-layered specimen, HCCT3L.

showed a peak crushing force higher than that of columnar tube series HCCT1L and ACT0L as a result of the absence of the circumferential delamination in collapse mode. This composite tube (HCCT2L) showed a continuous increase in average crushing force as a result of adding two layers in composite overwrapped thickness. It behaved increasingly linearly at the beginning up to peak crushing force. It also showed that the fluctuating force influenced the longitudinal cracks of stationary hinges and failed to plastically fold the ACT. The composite layup or overwrap thickness of glass fiber skin influenced the rising slope of the curve. The specimen collapse commenced, and cracks were formed along the circumference at the top wall up to the middle wall of the specimen. This phenomenon occurred because the crushing force was higher than the threshold of the specimen. This phenomenon necessitated the sharp crush force reduction to continue the test. Based on the observation of the progressive failure, it effectively improved the average crushing force and in crashworthy capacity of the HCCT after a deformation length of 80 mm.

Fig. 9 shows the representative photographs of the deformation shapes obtained through the quasistatic crush test of three-layered epoxy-glass fiber HCCT, namely, HCCT3L. The crushing performance of HCCT3L was completely different from that of HCCT2L and HCCT1L. Fig. 9(a) illustrates that the hybrid columnar tube HCCT3L showed uniform crushing force with a catastrophic failure mode in the composite columnar tube and progressive deformation mode in the ACT because the two materials were separated at the interface. The initial phase of crushing force showed progressive crushing of triggering profile. However, a sudden growth of cracks fiber was observed immediately after the crushing force of the triggering profile, and these cracks propagated along the columnar length. Hybrid columnar tubes have an energy absorbing capacity that is equal to the combined energy absorbing capacities of pure aluminum and composite columnar tubes. After circumferential delamination, primary longitudinal cracks developed at four sharp corners as a result of stress concentrations. Each side of HCCT was split into petals that

moved inward and outward. The stationary cracks formed at the interface locations from one roving to another. HCCT3L lost its crushing force bearing capacity in the later crushing phases because of stationary crack propagation. The wedge was developed through crosswind fibers. It was larger than that in the aforementioned two kinds of HCCTs. The collapse mode of HCCT3L was stable. According to the observation of the failure mode, the aluminum tube wrapped with three layers of composite material effectively improved energy absorption capacity. HCCT3L was crushed with the stable post-buckling failure mode. The wrapped composite material was constrained into folds of the aluminum tube. During deformation of the aluminum tube, the composite material played an important role in preventing the aluminum tube from folding. The failure of the HCCT was in progress given that the inner ACT could function as crack initiator and controller.

The relationship between axial crush force and deformation curve of HCCT3L is shown in Fig. 9(b). The curve indicates that the crushing force linearly increased and then dropped immediately after the peak crush force. The specimen failure occurred at the trigger location, and crushing force capacity decreased. The decreasing crushing force capacity was consumed by lamina bending followed by the breakage of resin bonds. The separation of plies from one another occurred at the middle shell thickness of the columnar tube wall because of the delamination process. Crushing force value linearly increased after triggering profile. Moreover, lamina bending completely failed within the specimen, and the specimen settled in the flat plate at the bottom. The crushing force value continued to increase until the maximum value was reached. At this point, specimen buckling started and the crushing force value decreased abruptly. HCCT3L also showed global buckling from the top of the wall structure. The fold formations became difficult as a result of adding epoxy- glass fiber layers in the overwrapped thickness. The composite layup evidently plays a significant role in the selection of the crashworthy capacity. On the contrary, high crashworthy capacity could be obtained from the HCCT with three-layer epoxy-glass fiber composite material. Hence, the performance of HCCT3L is more efficient than that of other HCCTs, namely, HCCT2L and HCCT1L. Therefore, HCCT3L is the best choice in the energy absorbing system design.

As mentioned in the previous section, the crashworthiness parameters were calculated; these parameters include maximum peak crush resistive force (P_{max}), specific resistive force ($P_{specific}$) (i.e., the ratio of maximum peak crush resistive force [P_{max}] to the cross-sectional area of the columnar tube specimen), absorbed crash energy (E_{total}) (i.e., the area under force deformation curve), specific energy ($E_{specific}$) (i.e., the ratio between absorbed energy [E_{total}] and crushed columnar specimen mass [m_1], which is the crushed volume of specimen multiplied with density of composite), mean crush resistive force (P_{mean}) (i.e., the ratio of absorbed energy [E_{total}] to the total axial deformation length [d_{total}]), and crush resistive force efficiency (η_c). The distinct deformation modes of each samples were also identified and examined to determine the failure mechanisms that are responsible for the transient deformation process of hybrid aluminum-composite columnar, and the obtained results are tabulated in Table 2.

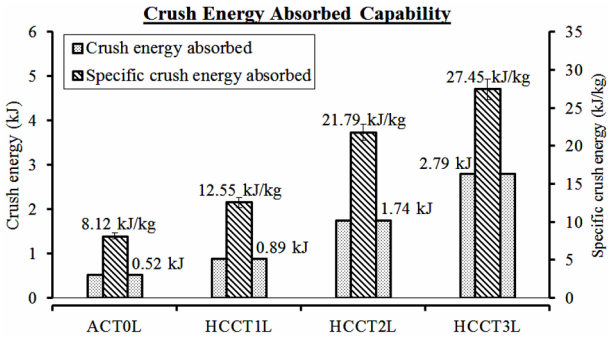

Fig. 10. Comparisons of mean crush force, maximum crush force, and crush force efficiency for ACTs.

3.3 Crashworthiness capacity

As previously referred in Figs. 6(b)-9(b) (Middle), the crushing force started at a critical point called *folding initiation force* or *maximum crushing force*, and then the crushing force traveled along the columnar tube structures. Both folding initiation force and mean crushing force of HCCT were significantly higher than those of ACT. Increased peak crushing force and mean crushing force were associated with the addition of a number of composite layers. This finding clearly indicated that the number of composite layup in the columnar tube wall thickness of tested specimens significantly influenced the peak crushing force.

The average result of crush performance properties of HCCTs with different overwrap thickness is shown in Fig. 10. The values of maximum crushing force and mean crushing force of HCCT3L are significantly higher than those of one- and two-layer laminations. The folding initiation force decreased as the number of layers decreased from three-layer overwraps to one-layer overwrap. The peak crushing force and the mean crushing force were nearly constant in the overwrap thickness of epoxy-glass fiber skins. This constant presented the critical thickness of hybrid epoxy-glass fiber columnar tubes.

Attention should be directed to the crushing force efficiency of the energy absorber device to evaluate its crashworthiness capacity. The diagram depicted in Fig. 10 includes the maximum crushing force, mean crushing force, and crushing force efficiency. As mentioned, crushing force efficiency is an important measurement of crush performance properties of HCCTs. The ratio of mean crushing force and maximum crushing force is a considerable value to present the collapse mechanism of composite, namely, progressive collapse or catastrophic collapse. The high value of crushing force efficiency in the HCCTs compared with that of the ACT proved that catastrophic collapse occurred in all hybrid epoxy-glass

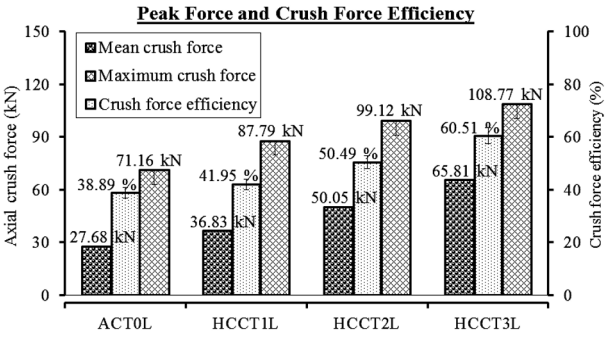

Fig. 11. Comparisons of total crush energy and specific crush energy absorbing properties of ACTs.

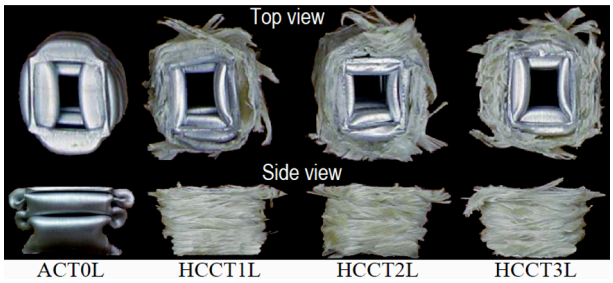

Fig. 12. Final collapsed shape of extruded aluminum columnar and epoxy-glass fiber skin overwrapped hybrid columnar profiles.

fiber columnar tubes. Catastrophic collapse was affected by overwrap thickness of the specimen. The values of maximum and mean crushing forces obtained by HCCT3L are slightly higher than those obtained by HCCT2L and HCCT1L. Therefore, the crashworthy capacity maximum crushing force, mean crushing force, and crushing force efficiency of all HCCTs were significantly higher than those of ACT.

3.4 Level of crush energy and specific energy absorptions

As previously shown in Figs. 6(c)-9(c) (Bottom), the comparison of the amount of crush energy and specific crush energy absorbing properties of extruded ACT with those properties of HCCTs for ~80 mm of quasistatic axial crushing force is illustrated in Fig. 11. The value of crush energy absorbing capacity of a structure depends on the area under the axial crush force-deformation curve. Fig. 11 also shows that energy absorption of HCCTs was significantly higher than that of aluminum tube. The highest energy absorption by HCCTs was observed at three-layered composite materials, and this value decreased with a decreasing number of layers. The energy absorption was also a function of the number of layers associated with aluminum thickness in the HCCT. The energy absorption of the hybrid columnar tubes relative to the aluminum tube increased with an increasing number of layers. Specific crush energy absorption is defined as the ratio of the energy absorbed per unit mass of the columnar tube. The thickness of specimens had the reverse effect on specific crush energy. Increasing the number of layers had a direct effect on increasing the specific crush energy. Specific crush energy in HCCTs showed improvement with the addition of a number of epoxy-glass fiber layers or composite overwrap. Therefore, the epoxy-glass fiber layers or composite overwrapped thicknesses played a major role in determining the enhancement energy absorption capacity. Consequently, columnar tubes with increased crush force showed increased crush energy and specific crush energy absorption.

According to Fig. 11, the energy absorption capacity increased to 24.8% once overwrap thickness was increased from 2.78 mm (1-layer epoxy-glass fiber material) to 3.47 mm (2-layer epoxy-glass fiber material) and increased to 62.2% once overwrap thickness increased from 2.78 mm to 4.51 mm (3-layer epoxy-glass fiber material). The results indicated that the capacity of energy absorption in HCCTs depended on the number of layers of columnar tubes. The HCCT with three layers in the overwrap composite thickness could absorb a large amount of energy. Hence, the large overwrap composite thickness of HCCTs influenced the crushing force. According to the investigation, the glass fiber-epoxy composite overwrap associated with ACT increased significant amount of specific crush energy absorption compared with ACT. The energy absorption capacity HCCT3L was higher than that of other columnar tube specimens. However, ACT0L without any epoxy-glass fiber material showed minimal specific crush energy absorption capacity. This finding showed that the weight is also an effective factor that influences specific crush energy absorption.

3.5 Collapse modes of HCCTs

In the crush tests, the barreling shape of the deformed specimen can function as a result of friction between the rigid platens and the specimen. This interfacial friction plays an important role on the collapse mode. Moreover, the deformation mode is characterized by depending on the relative friction value. The mode of collapse of aluminum tube shell and hybrid composite columnar shell was observed. Corresponding graphs that illustrate the axial crush force against crush deformation length dataset were recorded up to 67% (which is equal to total axial crushed distance of 80 mm) of the specimen through an automatic data acquisition device.

The modes of collapse for all aluminum and hybrid columnar tube specimens were analyzed experimentally and compared. The aluminum columnar shells formed axisymmetric elastic mode of buckling followed by plastic rolling toward loading axis on the end of the column. After elastic and plastic rolling, the symmetric mode of buckling changed into non-symmetric diamond modes of lobs. The formations of stationary cracks and several folds were also observed. A similar mode of collapse was observed in composite-wrapped columnar specimens. However, the size and position of diamond lobs differed from those of aluminum columnar shells. Fig. 12 shows comparison photographs of final collapse shapes ob-

tained from axial crush test of the hybrid tubes wrapped with the composite materials. Some fibers buckled toward the inner width, whereas the other fibers buckled toward the outer width. The matrix was nearly completely fractured and removed. Longitudinal cracks were developed between fibers along the length of the tube. The crosswind fibers were fractured up to the crush front.

3.6 Local crushing morphology

A detailed SEM analysis was concentrated over the laminate failure regions to understand clearly the characteristics of hybrid composite columnar shell during the axial crushing force. The overall crush morphology into laminate failure regions includes interlaminar/interlaminar crack propagation, frond bending, longitudinal splitting, flexural damage, and friction between laminates [21].

In this study, the crushing in failure mode was characterized by the wedge-shaped laminate cross section with multiple short or long interlaminar and longitudinal cracks that formed partial lamina bundles. One such failure of resin laminate was epoxy-glass fiber splitting. The epoxy-glass fiber/resin laminates split into two fronds during axial loading and were followed by laminate bending. The laminate bent further because of continuous axial crushing, thereby leading to local buckling. The buckled regions of the laminate started to delaminate from the aluminum surfaces. The fracture surfaces from all the samples were coated and examined by using an optical microscope (Philips, model: XL30) at magnification factors of 50-1000 times and voltage accelerations of 12 kV. The imaging software Motic Image was utilized to capture the image and analyze the fiber laminate failure modes. The image analysis shows that the epoxy-glass fiber laminate split into two divisions of fronds, which bent toward the columnar axis and away from the columnar axis. The former one was called internal frond, because it bent toward the axis of loading. The later one was external frond, which bent away from the axis of loading. In between the external and internal fronds of junctions, wedge-shaped fiber bundles were noticed. This wedge acted as a resisting member for the extension of axial crack.

Fig. 13 shows the microscopic details of lamina failure mode of HCCT3L columnar tube collapse. Fig. 13(a) illustrates the cross-sectional view, whereas Figs. 13(b)-(d) illustrate the SEM micrographs. The progressive failure was observed from top end of the columnar shell and propagates perpendicularly to the loading direction of rigid steel platen, i.e., around the circumference of the columnar shell. In the crack tip of the main central interwall crack (Point ① in Figs. 13(a) and (b)), matrix cleavages and debonded fibers were observed. Figs. 13(c) and (d) illustrate fracture surface of the warp and fill direction in the delamination region (Point ② in Fig. 13(b)). At point ②, the tube wall was in contact with the rigid steel platen and bent outward. Therefore, a mixture of various microscopic failure modes exists. Matrix squeezing via crushing force and fiber fracture bending force via rigid steel platen were also observed.

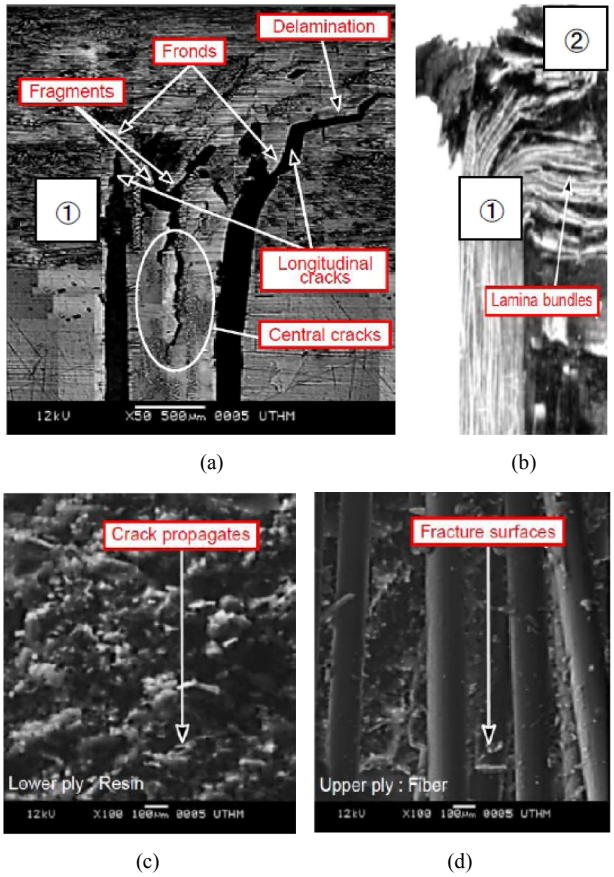

Fig. 13. SEM micrographs of crushing zone of hybrid composite tube showing fiber in failure modes: (a) crack tip of the main central interwall crack; (b) terminal view of epoxy-glass fiber laminate; (c) fracture surfaces of fill direction of epoxy-glass fiber laminate; (d) resin-rich carbon fiber in delamination region.

4. Conclusions

Repeated axial crush tests were conducted on aluminum HCCTs over a range of incident crush absorbed energies to determine their axial crush performance. The conclusions drawn from the experimental results are summarized as follows:

(i) The quasistatic axial crashworthy capacity of aluminum HCCTs can be improved with an overwrap thickness of epoxy-glass fiber skin.

(ii) The crush force and number of layers of the specimens play a major role in determining the rate of enhancement energy absorption and are dependent on stacking sequences.

(iii) The overall energy absorption mechanism of crushed HCCTs are further shown to be in the matrix crack and microcrack propagation, frond buckling, splitting, and friction between laminates or overwrap because of structure recovery from collapse.

(iv) Given that the folding pattern is asymmetric for all

HCCTs, the folding initiation force, crush force efficiency, and specific crush energy absorbed by HCCT3L are more efficient compared with other columnar tubes, namely, ACT0L, HCCT1L, and HCCT2L. The columnar tube HCCT3L is also the best choice in the design of an energy absorbing system that deals with square geometry tube structures, and it can be used in any structure.

(v) Crashworthiness parameters, such as maximum crush force, mean crush force, and crush energy absorption, and the changes of collapse category from catastrophic to progressive have improved significantly because of the use of number of layers.

(vi) This study also indicates that material parameters, such as the number of layers in the overwrap, and ACT wall thickness can be adjusted to influence the desired crush performance of hybrid columnar tube materials and structures.

(vii) Additional results for the microscopic analysis of crush resistance by SEM microscopy techniques were acquired to obtain a clear overview of the final collapse of the specimen.

Acknowledgment

The authors sincerely thank Kementerian Pendidikan Malaysia and Jabatan Pengajian Politeknik for providing Fundamental Research Grant Scheme - FRGS Vot P41 (Reference No. FRGS/1/2014/TK01/JPP/03/1) and the METALGLASS Company of Malaysia Sabah for supplying ACTs. Special thanks is extended to Engr. Stanley Gualin for his assistance in the experimental investigation and to the authorities of PKK, UTHM, UIAM, and UMS for their support and encouragement.

References

[1] A. Paluszny, *State of the art review of automobile structural crashworthiness*, Southfield, MI: American Iron and Steel Institute (1992).

[2] P. H. E. P. J. Thornton and R. A. Jeryan, Crash energy management in composite automotive structures, *International Journal of Impact Engineering*, 7 (1988) 167-180.

[3] S. Ramakrishna, Microstructural design of composite materials for crashworthy structural applications, *Materials & Design*, 18 (1997) 167-173.

[4] X. Liu and S. Mahadevan, Ultimate strength failure probability estimation of composite structures, *Journal of Reinforced Plastics & Composites*, 19 (2000) 403-426.

[5] I. Baran, C. C. Tutum, M. W. Nielsen and J. H. Hattel, Process induced residual stresses and distortions in pultrusion, *Composites Part B: Engineering*, 51 (2013) 148-161.

[6] I. Baran, C. C. Tutum and J. H. Hattel, Reliability estimation of the pultrusion process using the first-order reliability method (FORM), *Applied Composite Materials*, 20 (2013) 639-653.

[7] I. Baran, C. C. Tutum and J. H. Hattel, Probabilistic thermochemical analysis of a pultruded composite rod, *Proceedings of the 15th European conference on composite materials, ECCM-15*, Venice, Italy, 24-28 June (2012).

[8] I. Baran, C. C. Tutum and J. H. Hattel, The effect of thermal contact resistance on the thermosetting pultrusion process, *Composites Part B: Engineering*, 45 (2013) 995-1000.

[9] I. Baran, C. C. Tutum and J. H. Hattel, Optimization of the thermosetting pultrusion process by using hybrid and mixed integer genetic algorithms, *Applied Composite Materials*, 20 (2013) 449-463.

[10] P. Paruka and W. A. Siswanto, Axial impact performance of aluminium thin cylindrical tube, *Applied Mechanics and Materials*, 315 (2013) 1-5.

[11] H. C. Kim, D. K. Shin, J. J. Lee and J. B. Kwon, Crashworthiness of aluminum/CFRP square hollow section beam under axial impact loading for crash box application, *Composite Structures*, 112 (2014) 1-10.

[12] D. K. Shin, H. C. Kim and J. J. Lee, Numerical analysis of the damage behavior of an aluminum/CFRP hybrid beam under three point bending, *Composites Part B: Engineering*, 56 (2014) 397-407.

[13] A. H. Varma, J. M. Ricles, R. Sause and L. W. Lu, Seismic behavior and design of high-strength square concrete-filled steel tube beam columns, *Journal of Structural Engineering*, 130 (2) (2004) 169-179.

[14] G. Li, M. John and D. Maricherla, Experimental study of hybrid composite beams, *Construction and Building Materials*, 21 (2007) 601-608.

[15] D. Zangani, M. Robinson and A. G. Gibson, Progressive failure of composite hollow sections with foam-filled corrugated sandwich walls, *Applied Composite Materials,* 14 (2007) 325-342.

[16] A. Ragalyi and P. K. Mallick, Crashworthiness of aluminum-composite hybrid crush tubes containing filament-wound over-wraps, *Proceedings of SAMPE-ACCE-DOE-SPE Midwest Advanced Materials and Processing Conferences*, Dearborn, MI (2000) 420-426.

[17] M. Y. Huang, Y. S. Tai and H. T. Hu, Numerical study on hybrid tubes subjected to static and dynamic loading, *Applied Composite Materials*, 19 (2012) 1-19.

[18] H. El-Hage, P. K. Mallick and N. Zamani, A numerical study on the quasi-static axial crush characteristics of square aluminum-composite hybrid tubes, *Composite Structures*, 73 (2006) 505-514.

[19] J. Bouchet, E. Jacquelin and P. Hamelin, Dynamic axial crushing of combined composite aluminium tube: the role of both reinforcement and surface treatments, *Composite Structures*, 56 (2002) 87-96.

[20] M. David, A. F. Johnson and H. Voggenreiter, Analysis of crushing response of composite crashworthy structures, *Applied Composite Materials*, 20 (2013) 773-787.

[21] K. C. Shin, J. J. Lee, K. H. Kim, M. C. Song and J. S. Huh, Axial crush and bending collapse of an aluminum/GFRP hybrid square tube and its energy absorption capability, *Composite Structures*, 57 (2002) 279-287.

[22] H. W. Song, Z. M. Wan, Z. M. Xie and X. W. Du, Axial impact behavior and energy absorption efficiency of com-

posite wrapped metal tubes, *International Journal of Impact Engineering*, 24 (2000) 385-401.
[23] E. H. Hanefi and T. Wierzbicki, Axial crush resistance and energy absorption of externally reinforced metal tubes, *Composites: Part B*, 27B (1996) 387-394.
[24] M. A. Jimenez, E. Larrode and D. Revuelta, Effect of trigger geometry on energy absorption in composite profiles, *Composite Structures*, 48 (1-3) (2000) 107-111.
[25] S. Palanivelu, W. V. Paepegem, J. Degrieck, J. V. Ackeren, D. Kakogiannis, D. V. Hemelrijck, J. Wastiels and J. Vantomme, Experimental study on the axial crushing behaviour of pultruded composite tubes, *Polymer Testing*, 29 (2010) 224-234.
[26] H. Ghasemnejad, B. R. K. Blackman, H. Hadavinia and B. Sudall, Experimental studies on fracture characterizations and energy absorption of GFRP composite box structures, *Composite Structures*, 88 (2009) 253-261.
[27] W. C. Hwang, K. S. Lee, Y. J. Yang and I. Y. Yang, An experimental study on the optimum collapse characteristics of composite structural member under impact loading, *International Journal of Precision Engineering and Manufacturing*, 12 (3) (2011) 521-526.
[28] P. Paruka, M. K. M. Shah and M. A. Mannan, Influence of axial and oblique impact loads on crush response of square tube structures made with FRP pultruded composites, *Procedia Engineering*, 68 (2013) 572-578.
[29] N. Jones, *Structural impact*, Paperback Edition 1997, Cambridge: Cambridge University Press (1989).
[30] E. Mahdi, A. S. M. Hamouda, A. S. Mokhtar and D. L. Majid, Many aspects to improve damage tolerance of collapsible composite energy absorber devices, *Composite Structures*, 67 (2005)175-187.

Perowansa Paruka is a technical lecturer (Engineer) at the Department of Mechanical Engineering in Politeknik Kota Kinabalu (PKK), Sabah, Malaysia. He is currently an M.Phil. student of Mechanical Engineering at Universiti Malaysia Sabah (UMS). He earned his Bachelor of Science degree in Engineering (Hons) in Universiti Tun Hussein Onn Malaysia, Johor, Malaysia. His research interest is automotive computational mechanics, including FEM-based crash/impact simulation.

Waluyo Adi Siswanto is an associate professor of the faculty of mechanical and manufacturing engineering at Universiti Tun Hussein Onn Malaysia (UTHM). He earned his Ph.D. in Mechanical Engineering (2000) at the Royal Melbourne Institute of Technology (RMIT) University. His research interests include computational mechanics and FEM-based simulations.

Md Abdul Maleque is an associate professor of Kuliyyah of Engineering at Universiti Islam Antarabangsa Malaysia (UIAM). He earned his Ph.D. in Mechanical Engineering (2001) at Universiti Malaya, Kuala Lumpur, Malaysia. His research interests include computational mechanics, advanced composite materials, and materials for automotive and energy.

Mohd Kamal Mohd Shah is a senior lecturer of the Engineering faculty at Universiti Malaysia Sabah (UMS). He earned his Ph.D. in Mechanical Engineering (2012) at UMS, Kota Kinabalu, Sabah, Malaysia. His research interests are computational mechanics, including advanced composite and smart materials.